



Isomer distribution and structure of (2,2'-biphenyldiolato)bis(β-diketonato)-titanium(IV) complexes: A single crystal X-ray, solution NMR and computational study

Annemarie Kuhn, Tsietsi A. Tsotetsi, Alfred Muller, Jeanet Conradie*

Department of Chemistry, University of the Free State, Nelson Mandela Drive, Bloemfontein 9301, South Africa

ARTICLE INFO

Article history:

Received 15 September 2008

Received in revised form 2 February 2009

Accepted 6 February 2009

Available online 20 February 2009

Keywords:

β-Diketonato

Titanium

DFT

Isomer distribution

Structure

ABSTRACT

Novel dichlorobis(β-diketonato)titanium(IV) $\text{Ti}(\text{C}_6\text{H}_5\text{COCHCOR})_2\text{Cl}_2$ and (2,2'-biphenyldiolato)bis(β-diketonato)titanium(IV) $\text{Ti}(\text{C}_6\text{H}_5\text{COCHCOR})_2\text{biphen}$ complexes with $\text{R} = \text{CH}_3$, C_6H_5 and CF_3 , are synthesized and characterized by X-ray crystallography and further physical methods. There is a good agreement between DFT calculated and experimental structural data. A configurational analysis gives a calculated isomer distribution that is in agreement with the experimental data derived from low temperature ^1H NMR spectroscopy. The $\text{Ti}(\text{C}_6\text{H}_5\text{COCHCOR})_2\text{biphen}$ complexes exhibit high hydrolytic stability.

© 2009 Elsevier B.V. All rights reserved.

1. Introduction

Complexes of titanium(IV) are widely studied for a variety of purposes, mainly serving as catalyst in different organic reactions [1] as well as for antitumor activity [2]. Two monomeric Ti(IV) complexes have qualified for clinical trials on antitumor activity: $\text{Ti}(\text{ba})_2(\text{OEt})_2$ (budotitane, Hba = benzoylacetone) [3] and TiCp_2Cl_2 (titanocene dichloride) [4], but clinical phase II and phase III have been stopped mainly as a consequence of problems with the galenic formulation of the compound [5]. Since no information on the isomer distribution of budotitane in the galenic formulation used for the tests of the anticancer activity is available, it is of importance to understand the spatial arrangement of the monomeric Ti complex and which of the five possible isomers of six-coordinate octahedrally configured $\text{Ti}(\text{ba})_2\text{X}_2$ ($\text{X} = \text{OEt}$ or Cl) complexes exhibit anticancer activity. The decomposition of titanocene dichloride and budotitane in aqueous solutions impeded mechanistic investigations, lowered their efficiency and ultimately resulted in failure of clinical trials. Thus producing titanium(IV) complexes exhibiting enhanced water stability, is extremely valuable.

Molecular mechanics (MM) has successfully been used to calculate the isomer distribution of budotitane [6]. The main disadvantage of molecular mechanics is the lack of available parameters for many compound types. Also, since electrons and orbitals are not used in the MM method, we cannot study chemical reactions or

predict reactivity of molecules with MM. With the improvement of computational methods and computer power, methods such as density functional theory (DFT) is computationally less demanding and can thus conveniently be used for the calculation of molecular geometry, isomer distribution as well as electronic properties of the molecule.

Utilizing a Single Crystal X-ray, variable temperature ^1H and ^{19}F NMR and DFT computational chemistry techniques, this paper describes the isomeric abundance of a series of octahedral $\text{Ti}(\beta\text{-diketonato})_2\text{Cl}_2$ and $\text{Ti}(\beta\text{-diketonato})_2\text{biphen}$ -complexes, biphen = biphenolato, β-diketonato = $\text{C}_6\text{H}_5\text{COCHCOR}$ with $\text{R} = \text{CH}_3$, C_6H_5 and CF_3 . The novel $\text{Ti}(\beta\text{-diketonato})_2\text{biphen}$ complexes, not previously reported, exhibit high resistance towards hydrolysis.

2. Experimental

2.1. Materials and apparatus

Solid reagents used in preparations (Merck, Aldrich and Fluka) were used without further purification. Liquid reactants and solvents were distilled prior to use; water was doubly distilled. Organic solvents were dried according to published methods [7].

2.2. Synthesis of $\text{Ti}(\beta\text{-diketonato})_2\text{Cl}_2$ complexes 1–3

The $\text{Ti}(\beta\text{-diketonato})_2\text{Cl}_2$ complexes were synthesized according to published methods for $\text{Ti}(\text{CH}_3\text{COCHCOC}_6\text{H}_5)_2\text{Cl}_2$ **1** and $\text{Ti}(\text{C}_6\text{H}_5\text{COCHCOC}_6\text{H}_5)_2\text{Cl}_2$ **2** [8,9].

* Corresponding author. Tel.: +27 51 401 2194; fax: +27 51 444 6384.

E-mail address: conradj.sci@ufs.ac.za (J. Conradie).

Ti(C₆H₅COCHCOCF₃)₂Cl₂ **3**: Yield: 16.0%. M.p. > 250 °C. ¹H NMR (δ/ppm, CDCl₃): 7.05 (2H, s, tfbaH), 7.58 (4H, t, PhH), 7.77 (2H, t, PhH), 8.11 (4H, br, PhH). ¹⁹F NMR (δ/ppm, CDCl₃): –74.50 (6F, br, CF₃). Elemental Anal. Calc.: for TiC₂₀H₁₂O₄Cl₂F₆ C, 43.8; H, 2.2. Found: C, 43.8; H, 2.1%.

2.3. Synthesis of Ti(β-diketonato)₂biphen complexes **4–6**

To stirred solution of 2,2'-biphenyldiol (0.186 g, 1 mmol in 15 ml CH₃CN) at RT, a solution of Ti(C₆H₅COCHCOR)₂Cl₂ (1 mmol in 15 ml CH₃CN) was added dropwise at room temperature with an immediate colour change. After refluxing for 4.6 h, the reaction mixture was cooled and solvent evaporated until it was dry. The residue was washed in MeOH to dissolve unreacted biphenol in **4** and **5**. Pure product was obtained recrystallization from dichloromethane/*n*-hexane and stored under N₂ atmosphere.

Ti(C₆H₅COCHCOCH₃)₂biphen **4**: Yield: 0.113 g (20.4%). M.p. > 250 °C. ¹H NMR (δ/ppm, CDCl₃): 2.20 (6H, s, CH₃), 6.48 (2H, s, baH), 7.02 (2H, d, biphenH), 7.08 (2H, t, biphenH), 7.32 (2H, t, biphenH), 7.38 (4H, t, PhH), 7.45 (2H, d, biphenH), 7.50 (2H, t, PhH), 7.81 (4H, d, PhH). Elemental Anal. Calc. for TiC₃₂H₂₆O₆: C, 69.3; H, 4.7. Found: C, 69.3; H, 4.6%.

Ti(C₆H₅COCHCOCH₃)₂biphen **5**: Yield: 0.154 g (22.3%). M.p. 244.93 °C. ¹H NMR (δ/ppm, CDCl₃): 7.11 (2H, d, biphenH), 7.14 (2H, t, biphenH), 7.18 (2H, s, dbmH), 7.35–7.57 (16H, m, aromaticH), 7.95 (8H, d, PhH). Elemental Anal. Calc. for TiC₃₈H₂₆O₆S₂: C, 66.1; H, 3.8. Found: C, 66.0; H, 3.7%.

Ti(C₆H₅COCHCOCF₃)₂biphen **6**: Yield: 0.106 g (24.6%). M.p. > 250 °C. ¹H NMR (δ/ppm, CDCl₃): 6.89 (2H, s, tfbaH), 7.02 (2H, d, biphenH), 7.16 (2H, t, biphenH), 7.36 (2H, t, biphenH), 7.47 (4H, t, PhH), 7.52 (2H, d, biphenH), 7.64 (2H, t, PhH), 7.91 (4H, d, PhH). ¹⁹F NMR (δ/ppm, CDCl₃): –75.03 (6F, br, CF₃). Elemental Anal. Calc. for TiC₃₂H₂₀O₆F₇: C, 58.0; H, 3.0. Found: C, 57.8; H, 3.0%.

2.4. Spectroscopy and spectrophotometry

NMR measurements at 25 °C were recorded on a Bruker Avance II 600 NMR spectrometer [¹H (600.130 MHz), ¹⁹F (564.686 MHz)]. The chemical shifts were reported relative to SiMe₄ (0.00 ppm) for ¹H and relative to CFCl₃ (0.00 ppm) for ¹⁹F. Positive values indicate downfield shift.

2.5. X-ray crystal structure determination

Crystals of Ti(C₆H₅COCHCOCH₃)₂biphen (**4**) were obtained from recrystallization in chloroform. X-ray intensity data for **2** was measured on a Bruker X8 Apex II 4 K CCD area detector, equipped with a graphite monochromator and Mo Kα fine-focus sealed tube (λ = 0.71073 Å) operated at 1.5 kW power (50 kV, 30 mA). The detector was placed at a distance of 3.75 cm from the crystal. Sample temperature was kept constant at 100(2) K using an Oxford 700 series cryostream cooler.

The initial unit cell and data collection of **2** were achieved by the APEX2 software [10] utilizing COSMO [11] for optimum collection of more than a hemisphere of reciprocal space. A total of 1149 frames were collected with a scan width of 0.5° in φ and ω with an exposure time of 60 s per frame. The frames were integrated using a narrow frame integration algorithm and reduced with the Bruker SAINTPLUS and XPREP software [12] packages, respectively. Analysis of the data collections showed no significant decay during the data collection. Data were corrected for absorption effects using the multi-scan technique SADABS [13].

The structure was solved by the direct methods package SIR97 [14] and refined using the WINGX software package [15] incorporating SHELXL [16]. The largest peaks on the final difference electron

densities and the deepest holes were all within 1 Å from non-hydrogen atoms which presented no physical meaning in the final refinements. Aromatic protons were placed in geometrically idealized positions (C–H = 0.95 Å) and constrained to ride on their parent atoms with U_{iso}(H) = 1.2U_{eq}(C). Initial positions of the methyl protons were obtained from a Fourier difference map and refined as fixed rotors with U_{iso}(H) = 1.5U_{eq}(C) and C–H = 0.98 Å.

Atomic scattering factors were taken from the International Tables for Crystallography Volume C [17]. The molecular plot was drawn using the DIAMOND program [18] with a 30% thermal envelope probability for non-hydrogen atoms. Hydrogen atoms were drawn as arbitrary sized spheres with a radius of 0.135 Å.

2.6. Theoretical approach

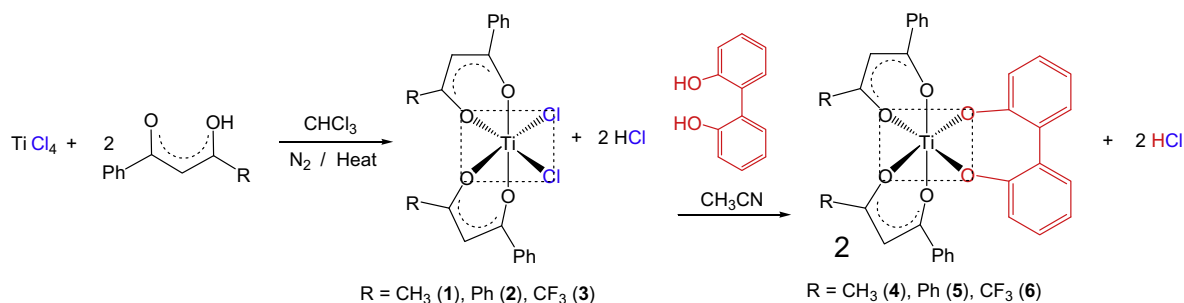
Density Functional Theory (DFT) calculations were carried out using the Amsterdam Density Functional 2007 (ADF) program system [19] with the PW91 (Perdew–Wang, 1991) exchange and correlation functional [20]. The TZP (Triple ζ polarized) basis set, a fine mesh for numerical integration (5.2 for geometry optimizations and 6.0 for frequency calculations), a spin-restricted (gas-phase) formalism and full geometry optimization with tight convergence criteria as implemented in the ADF 2007 program, were used. The accuracy of the computational method was evaluated by comparing the root-mean-square deviations (RMSD's) between the optimized molecular structure and the crystal structure, using the non-hydrogen atoms in the molecule. RMSD values were calculated using the “RMS Compare Structures” utility in ChemCraft Version 1.5 [21]. Whether artificially generated atomic coordinates or coordinates obtained from X-ray crystal data were used in the input files, optimizations for each compound resulted in the same minimum energy optimized geometry. Optimized structures were verified as a minimum through frequency calculations.

3. Results and discussion

3.1. Synthesis and identification of complexes

The dichlorobis(β-diketonato)titanium(IV), Ti(C₆H₅COCHCOR)₂Cl₂ with R = CH₃ (ba, **1**), C₆H₅ (dbm, **2**) and CF₃ (tfba, **3**) complexes were prepared by treating TiCl₄ with 2 equiv. of the appropriate β-diketone and isolated and purified by recrystallisation before use [7,8], see Scheme 1. The low yield obtained for the more acidic complex **3** (16% versus 80% for **1** and **2**) may be attributed to the electron withdrawing capability of the CF₃ groups making the β-diketone a poorer electrophile, thus making complex formation more difficult. Another contributing factor may be the titanium–fluorine single bond energy of 581 kJ mol^{−1} that is higher than that of the titanium–oxygen single bond, (478 kJ mol^{−1}) [22] favouring Ti–F bond formation, leading to side products and a lower yield of **3**. Products **1–3** were stored under an argon atmosphere since the Ti(β-diketonato)₂Cl₂ complexes are highly susceptible to hydrolysis. Complex **3** with a CF₃ containing β-diketonato is considerably less stable with respect to hydrolysis than the analogous complexes **1** and **2**, both in the solid state and in solution. The hydrolytic stability increases in the order Ti(tfba)₂Cl₂ ≪ Ti(dbm)₂Cl₂ < Ti(ba)₂Cl₂ [8]. Keppler and Heim evaluated the rate of hydrolysis (determined by the development of turbidity of the solution as a result of the precipitation on TiO₂), showing that complex **1** precipitates within 10 s when dissolved in dry CH₃CN treated with 0.01% water [23].

The (biphenyldiolato)bis(β-diketonato)titanium(IV), Ti(C₆H₅COCHCOR)₂(biphen) with R = CH₃ (ba, **4**), C₆H₅ (dbm, **5**) and CF₃ (tfba, **6**) complexes were obtained by the substitution of the bidentate biphenol ligand for the two monodentate Cl[−] ligands in Ti(β-diketonato)₂Cl₂, following a synthetic route similar to the one pub-



Scheme 1. Synthetic route for the synthesis of $\text{Ti}(\beta\text{-diketonato})_2\text{Cl}_2$ and $\text{Ti}(\beta\text{-diketonato})_2(\text{biphen})$.

lished by Rao et al. [24] for the reaction between $\text{Ti}(\text{CH}_3\text{COCHC}-\text{OCH}_3)_2\text{Cl}_2$ and 1,1'-methylene-2-naphthol, see Scheme 1. The biphenolato complexes **4–6** exhibit a high hydrolytic stability and are “air stable” for more than 3 years. The solution stability was tested under the same conditions as Keppler and Heim, i.e., 0.01% water/ CH_3CN , and it was found that the biphenolato complexes **4–6** do not precipitate within 6 weeks.

3.2. X-ray structure of (**4**)

A molecular diagram showing the numbering scheme of the title compound $\text{Ti}(\text{ba})_2\text{biphen}$ (**4**) is presented in Fig. 1a. Crystal data and details for data collections and refinements are summarized in Table 1. Selected bond lengths and angles for the molecule are listed in Table 2.

The compound $\text{Ti}(\text{ba})_2\text{biphen}$, **4**, crystallizes in the non-centrosymmetric trigonal space group, $P3_221$ with $Z = 3$, resulting in only half the molecule necessary for the asymmetric unit as it is situated on a twofold rotational axis. The $\text{Ti}(\text{ba})_2\text{biphen}$, **4**, structure consists of an octahedrally coordinated titanium atom with all three ligands acting as bidentate. The octahedral coordination around titanium is distorted to accommodate the three chelated li-

gands, i.e., the two six-membered benzoylacetonato and seven-membered biphenolato rings. The O–Ti–O bond angles vary from 83° to 97° compared to 90° in a perfect octahedron. The ligand O–Ti–O angle is 82.9° for the six-membered ba chelated ligand and 91.3° for the seven-membered biphenolato ring. The Ti–O bonds lengths in **4** are in the order $\text{Ti}-\text{O}_{\text{biphen}}$ (1.851 Å) < $\text{Ti}-\text{O}_{\text{ba axial}}$ (1.977 Å) < $\text{Ti}-\text{O}_{\text{ba equatorial}}$ (2.018 Å) as illustrated in Fig. 1b. The formal Ti–O single bond is 1.94–1.99 Å (Ti–O distances found in rutile, TiO_2 [25]) and Ti=O double bond is 1.61–1.68 Å [26]. Therefore, the shortest Ti–O distance is clearly shorter than one expected for a single bond, suggesting that this Ti–O bond possesses partial double bond character arising from donation of the electrons from the p_y and p_z filled oxygen orbitals to the empty titanium d orbitals [27]. The Ti–O_{ba} bonds *trans* to another ba oxygen, are shorter (1.977 Å) than those *trans* to the oxygen of the chelated dianion biphenolato ligand (2.018 Å).

Fig. 2 illustrates that the intermolecular molecular packing of **4** is mainly governed by edge-to-face C–H... π interactions [28], giving rise to the well-known herringbone packing motif illustrated in Fig. 3. Simple aromatic residues prefer to associate via enthalpically favourable edge-to-face C–H... π interactions [29]. The C–H... π interactions are (a) between biphen C–H and the

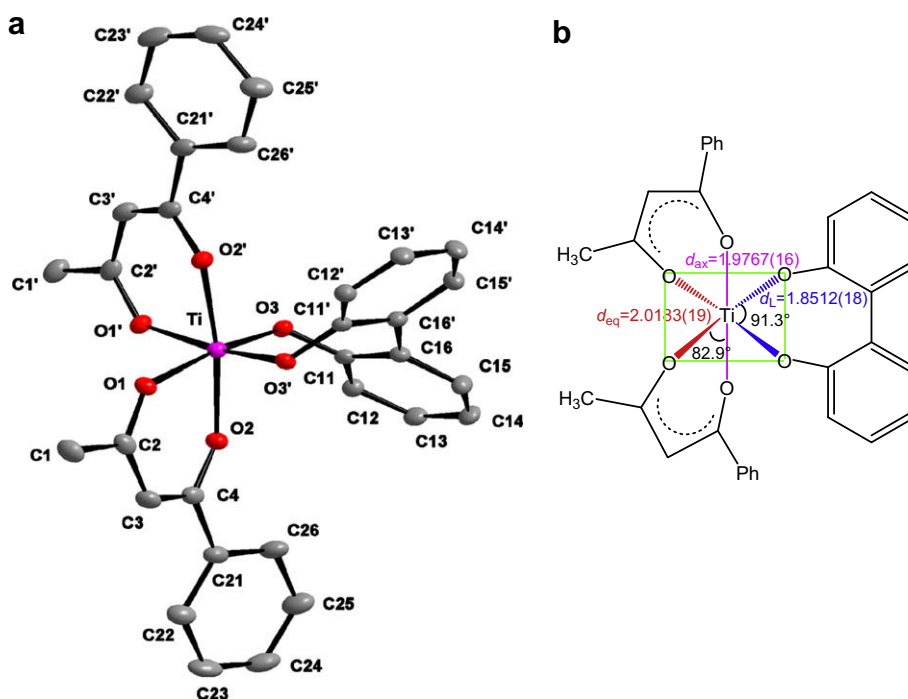


Fig. 1. (a) The molecular structure (30% probability displacement ellipsoids) of $\text{Ti}(\text{ba})_2\text{biphen}$ (**4**) showing the numbering scheme (primed labels indicate atoms generated by symmetry operations). (b) Diagram indicating coordination, distances (Å) and angles ($^\circ$) around the titanium centre.

Table 1
Crystal and structure refinement data for Ti(ba)₂biphen (**4**).

Formula	TiO ₆ C ₃₂ H ₂₆
Formula weight	554.43
Crystal colour/habit	Orange, cuboid
Crystal system	Trigonal
Space group	P3 ₂ 21
Unit cell dimensions	
<i>a</i> (Å)	8.91750(10)
<i>b</i> (Å)	8.91750(10)
<i>c</i> (Å)	29.2648(7)
α (°)	90
β (°)	90
γ (°)	120
Volume (Å ³)	2015.40(6)
<i>Z</i>	3
<i>D</i> _{calc} (Mg m ⁻³)	1.370
Temperature (°C)	-173
Wavelength (Å)	0.71073
Absorption coefficient (mm ⁻¹)	0.363
<i>F</i> (000)	864
Crystal size (mm)	0.40 × 0.22 × 0.20
θ Range for data collection (°)	2.09–28.30
Index ranges	-11 ≤ <i>h</i> ≤ 10, -11 ≤ <i>k</i> ≤ 11, -39 ≤ <i>l</i> ≤ 39
Reflections collected	25 594
Independent reflections	3326 [<i>R</i> _{int} = 0.0468]
Completeness to θ = 28.35 (%)	99.9
Absorption correction	Semi-empirical from equivalents
Max. and min. transmission	0.9309 and 0.8684
Refinement method	Full-matrix least-squares on <i>F</i> ²
Data/restraints/parameters	3326/0/178
Goodness-of-fit on <i>F</i> ²	1.242
Final <i>R</i> indices [<i>I</i> > 2σ(<i>I</i>)]	<i>R</i> ₁ = 0.0370, <i>wR</i> ₂ = 0.1001
<i>R</i> indices (all data)	<i>R</i> ₁ = 0.0552, <i>wR</i> ₂ = 0.1410
Largest difference in peak and hole (e Å ⁻³)	0.500 and -1.054

Table 2
Selected bond lengths [Å] and angles [°] for Ti(ba)₂biphen (**4**).

Ti–O(3)	1.8512(18)	O(2)–Ti–O(1)	82.90(7)
Ti–O(2)	1.9767(16)	O(3)#1–Ti–O(3)	91.34(11)
Ti–O(1)	2.0183(19)	O(3)–Ti–O(2)	88.90(7)
O(1)–C(2)	1.279(3)	O(2)#1–Ti–O(2)	171.52(11)
O(2)–C(4)	1.286(3)	O(3)–Ti–O(1)	171.80(7)
O(3)–C(11)	1.356(3)	C(2)–O(1)–Ti	133.06(17)
C(1)–C(2)	1.494(4)	C(4)–O(2)–Ti	133.87(17)
C(2)–C(3)	1.397(4)	O(1)–C(2)–C(3)	123.0(2)
C(3)–C(4)	1.392(4)	O(1)–C(2)–C(1)	116.9(2)
C(11)–C(16)	1.399(4)	C(4)–C(3)–C(2)	122.8(2)
C(16)–C(16)#1	1.493(5)	O(2)–C(4)–C(3)	122.9(2)

Symmetry transformations used to generate equivalent atoms: #1 *x* – *y*, –*y*, –*z* + 1/3.

phenyl substituents of the ba ligand of a neighbouring molecule creating infinite chains (3.257 Å), (b) between phenyl C–H and the phenyl substituent of the ba ligands of neighbouring molecule (3.309 Å) and (c) between the biphen C–H to both of the ba β-diketonato chelated ring systems of a neighbouring molecule (2.747 Å). Each of the four phenyl residues on one molecule of **4** is thus involved in at least two C–H···π interactions each, resulting in a stabilized interlocking 3D network.

3.3. isomer distribution

Unsymmetrically substituted Ti(β-diketonato)₂Cl₂ complexes can adopt three different *cis* and two *trans* orientations, see Scheme 2. The isomeric configuration has been defined by three *ci* or *trans* prefixes which specify first the relative position of the Cl-ligands, then the relative orientation of the phenyl groups, and finally the relative orientation of the R group on the β-diketonato ligand C₆H₅COCHCOR. It was argued on qualitative basis that the *cis* con-

figurations are more strained but preferred by electronic effects (pπ-dπ (t_{2g}) bonding of the β-diketonato ligands) [30]. According to NMR data as well as to force field calculation results [30], no configurations with the X ligands in the *trans* position are to be expected. Only those Ti(β-diketonato)₂X₂ complexes with the extremely bulky substituents such as iodide or *p*-dimethylamino-phenoxy as hydrolyzable group X have the *trans* form. The stereochemistry of the complexes can be inferred from NMR spectra. The *cis-cis-cis* isomer with no symmetry (point group C₁) may give rise to two methyl (only for **1**), two phenyl, and two ring proton resonances. Fluorine NMR spectra of *cis-cis-cis*-Ti(tfba)₂Cl₂ **3** should show two nonequivalent fluorine groups. The other four isomers, *cis-trans-cis* (point group C₂), *cis-cis-trans* (C₂), *trans-cis-cis* (C_{2v}) and *trans-trans-trans* (C_{2h}) all possess at least a two-fold axis and should give a single resonance for each type of group, see Scheme 2. Ti(β-diketonato)₂(biphen) complexes can adopt only a *cis* orientation, one possible *cis* isomer if the bound β-diketone in the 1 and 5-position has the same (symmetrically substituted) substituents, or three possible *cis* isomers if the bound β-diketone in the 1 and 5-position has different substituents (asymmetrically substituted), see Scheme 2. If a statistical distribution of three *cis* Ti(β-diketonato)₂(biphen) diastereomers exists, the relative equilibrium concentrations will be 50% *cis-cis-cis*, 25% *cis-cis-trans* and 25% *cis-trans-cis* and four equally intense terminal group resonances are expected.

At room temperature (294 K) only one single set of ¹H NMR signals was observed for compounds **1–3**. The resonance signal of the methine H is sharp, but the resonance signals of the methyl and Ph groups on the β-diketonato ligand are relatively broad due to rapid isomerization process (relative to the NMR time scale) which exchanges groups between non equivalent environments. For compounds **4–6** one single set of sharp signals was observed. The signals broaden and split up into three to four signals upon lowering in temperature. With further temperature lowering the split resonance signals sharpen up again.

Fig. 4 (left) illustrates the temperature dependence of selected proton resonances of Ti(ba)₂Cl₂ **1** and Ti(ba)₂(biphen) **4** in CDCl₃ solution. Below –40 °C, three proton-CH₃ resonances are observed at ca 2.2 ppm, which, on raising the temperature, collapse into a singlet as a result of the rapid isomerization process at RT which exchanges methyl groups between the four non equivalent environments of the three *cis* diastereoisomers. The two proton phenyl resonance of **4** at 7.81 ppm followed the same trend consistent with a rapidly interconverting changing of the phenyl groups of the three *cis* diastereoisomers. The ring methine proton (–CH=) resonance of **4** at 6.48 ppm also shows on temperature lowering at least three resonance peaks.

The ring methine proton (–CH=) resonance of both Ti(tfba)₂Cl₂ **3** and Ti(tfba)₂(biphen) **6** at 7.05 and 6.89 ppm, respectively (Fig. 4 right) shows four distinguishable signals of three different intensities at –60 °C, consistent with the existence of three *cis* isomers for both **3** and **6**, in CDCl₃ solution. The two lines of equal intensity are assigned to the *cis-cis-cis* isomer. More than one-CH= ring methine resonance in this slow exchange methine region was not previously observed for the Ti(β-diketonato)₂X₂ complexes. Ti(ba)₂X₂ complexes with X = F, Cl, Br, revealed a single although considerably broadened resonance signal even at –65 °C [8]. This may be due to poor NMR resolution or due to the fact that the exchange between the isomers was fast, even at low temperatures. Ti(ba)₂(O^{*i*}C₃H₇)₂ showed four resonances at –36.8 °C for the methyl resonance [31]. Low temperature ¹⁹F NMR of the CF₃ containing complexes **3** and **6** showed four sharp signals at –60 °C at ca –74 ppm due to the slow exchange (on NMR timescale) of the CF₃ groups between the four non equivalent environments. Unambiguous assignment of the two resonance signals of equal intensity at low temperature to the *cis-cis-cis*

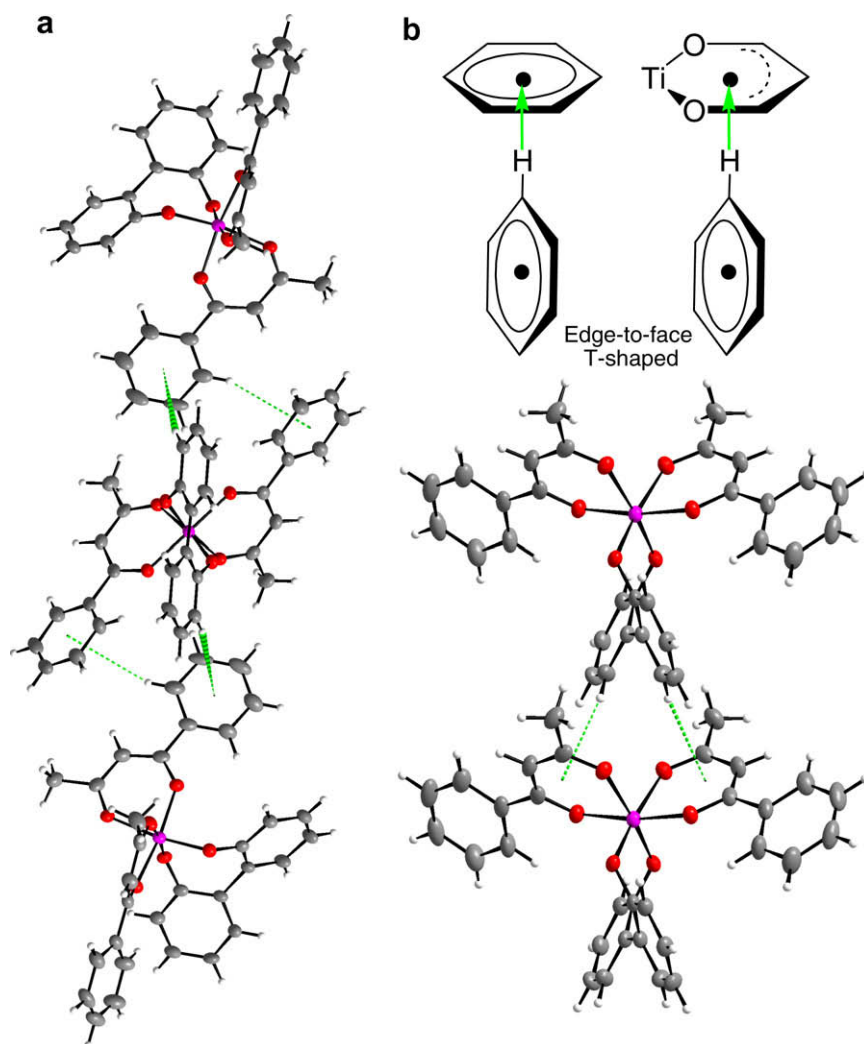


Fig. 2. Part of the packing diagram of $\text{Ti}(\text{ba})_2\text{biphen 4}$ showing intermolecular edge-to-face $\text{C-H}\cdots\pi$ interactions creating infinite chains. The $\text{C-H}\cdots\pi$ interactions are (a) between biphenyl C-H and ba phenyl of adjacent molecules, between ba C-H and ba phenyl of an adjacent molecule and (b) biphenyl C-H and the aromatic β -diketonato chelated ring systems in a neighbouring molecule.

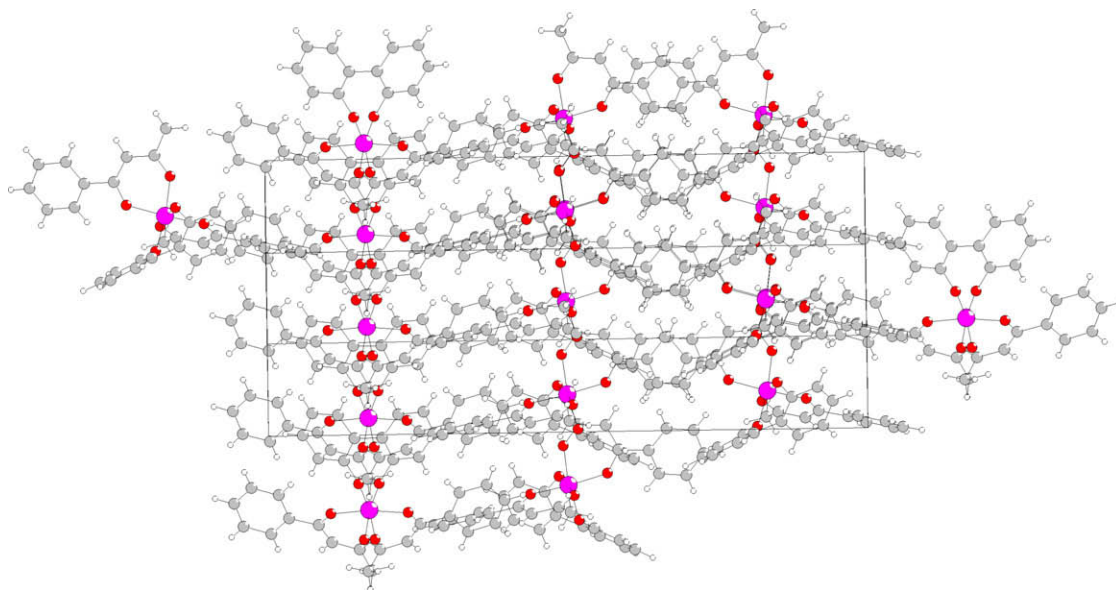
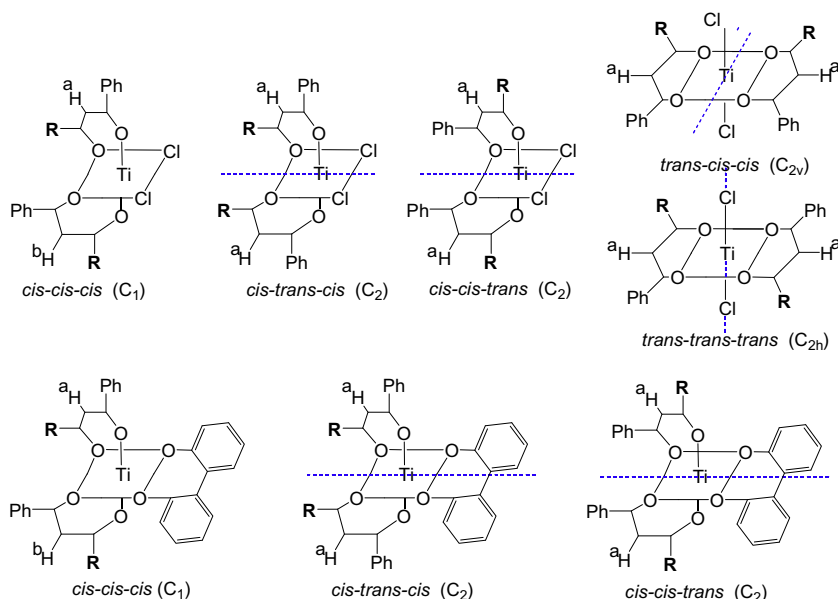


Fig. 3. Packing diagram showing the herringbone packing motif of $\text{Ti}(\text{ba})_2\text{biphen 4}$.



Scheme 2. The stereochemistry the isomers of asymmetrically substituted bis(β -diketonato) complexes of the type $\text{Ti}(\text{PhCOCHCOR})_2\text{Cl}_2$ and $\text{Ti}(\text{PhCOCHCOR})_2(\text{biphen})$: *cis-cis-cis* isomer (point group C_1 , give rise to two proton ^1H NMR resonances for each type of group), *cis-trans-cis* (point group C_2 , give a single resonance for each type of group), *cis-cis-trans* (C_2 , give a single resonance for each type of group), *trans-cis-cis* (C_{2v} , give a single resonance for each type of group) and *trans-trans-trans* (C_{2h} , give a single resonance for each type of group).

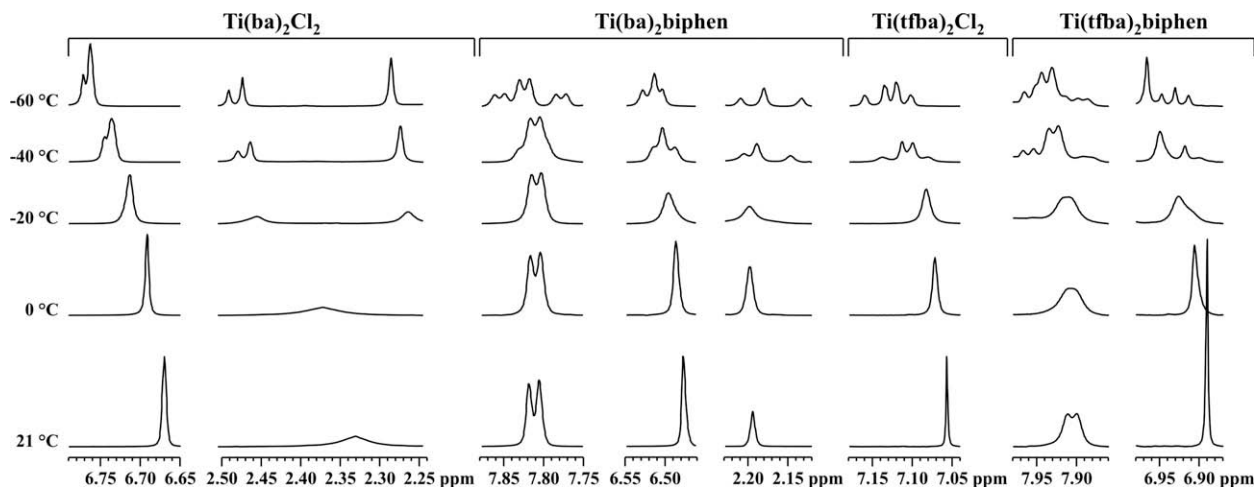


Fig. 4. Variable temperature ^1H NMR spectra of the indicated complexes showing selected phenyl (ca 7.8 ppm), methine (ca 6.5–7 ppm) and methyl (ca 2.2 ppm, only for **1** and **4**) resonances.

isomer of **3** and **6**, leads to an experimental isomer distribution of ca 35:25:40 and 20:60:20 for **3** and **6**, respectively, the first value belongs to the *cis-cis-cis* isomer. The isomer distribution of **3** and **6** thus deviates largely from the statistical value of 50:25:25.

3.4. Theoretical studies

Density functional theory (DFT) calculations were carried out on the different isomers of $\text{Ti}(\beta\text{-diketonato})_2\text{Cl}_2$ **1–3** and $\text{Ti}(\beta\text{-diketonato})_2(\text{biphen})$ **4–6**. The validity of the density functional method was obtained by comparing the calculated data with known single crystal X-ray diffraction structural data of **1** and **4**. The root-mean-square distances (RMSD) calculated for non-hydrogen atoms for the best three-dimensional superposition of calculated structures on experimental structures give a qualitative measure-

ment of the accuracy of the ground state geometry of the calculated structures. Excellent agreement between experimental and theoretical structures is obtained as reflected by the RMSD values of 0.061 and 0.041 Å for **1** and **4**, respectively. In Fig. 5, the superimposed calculated and solid state structures of **1** and **4** are presented. The bonds in **1** and **4** were reproduced by DFT calculations within 0.01–0.07 Å for Ti–O bonds, within 0.00–0.01 for O–C bonds and within 0.01–0.02 Å for C–C bonds from the experimental values. Since comparisons of experimental metal–ligand bond lengths with calculated bond lengths below a threshold of 0.02 Å are considered as meaningless [32], the computational method used thus gives a good account of experimental bond lengths. The O1–Ti–O2 angles were calculated accurately within 1.2°. Structural data computed with this computational method for related compounds may therefore, be presented with an extrapolative equally high degree of accuracy.

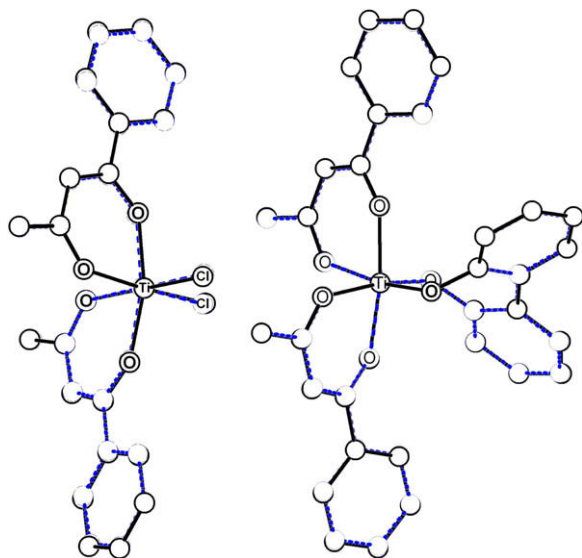


Fig. 5. An overlay view of the calculated (solid black) and the experimental (dashed blue) X-ray determined structure of $\text{Ti}(\text{ba})_2\text{Cl}_2$ (**1**) and $\text{Ti}(\text{ba})_2\text{biphen}$ (**4**). All unmarked molecules are C, H omitted for clarity.

Selected calculated geometrical parameters of the main isomers of complexes **1–6** are represented in Figs. 6–8. Three different Ti–O bond lengths as defined in Fig. 1b and summarized in Table 4 are found in complexes **1–6**. The longest Ti–O bonds, d_{eq} , are Ti–O $_{\beta}$ -diketonato bonds *trans* to d_L , a Ti–Cl or a Ti–O $_{\text{biphen}}$ bond. The shortest Ti–O bonds for **1–3** are axial Ti–O $_{\beta}$ -diketonato bonds *trans* to another d_{ax} Ti–O $_{\beta}$ -diketonato bond. The calculated Ti–O bond lengths in complexes **1–6** are in the order Ti–O $_{\text{biphen}}$ (1.82–1.87 Å) < Ti–O $_{\beta}$ axial (1.97–2.04 Å) < Ti–O $_{\beta}$ equatorial (2.05–2.12 Å). The different type of bond lengths did not change significantly when going from the one *cis* isomer to another.

The relative energies of the three *cis* isomers of each complex clearly highlight the geometry preferences and also enable a population analysis of the isomers by application of the Boltzmann equation. Especially pleasing is that the geometry of the lowest energy isomer of both **1** and **4** was the same as the isomer that crystallized from solution. The calculated isomer distribution is given in Table 3. The experimentally observed *cis–trans–cis* and *cis–cis–trans* populations are assigned according to the calculated isomer distribution. A generally good agreement is obtained between the experimentally observed isomer distribution and the calculated values.

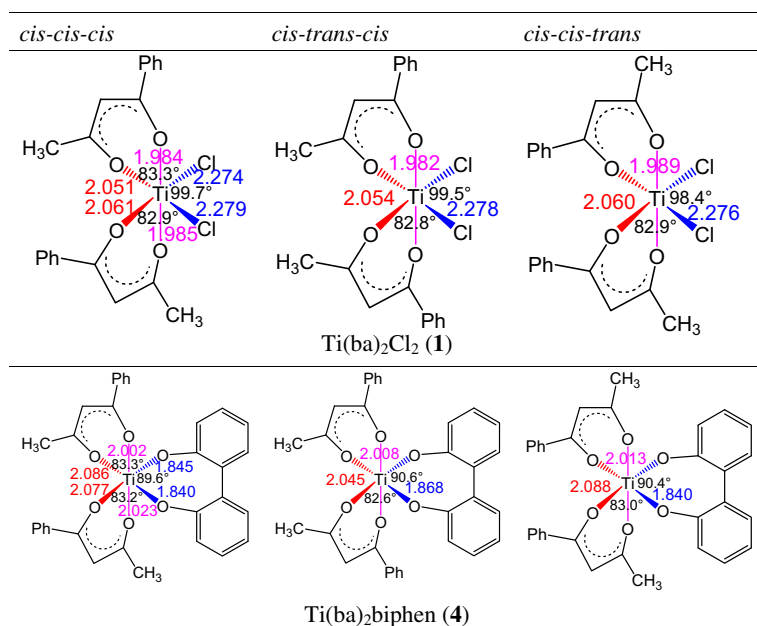


Fig. 6. Selected calculated bond lengths [Å] and angles [°] for $\text{Ti}(\text{ba})_2\text{Cl}_2$ and $\text{Ti}(\text{ba})_2\text{biphen}$.

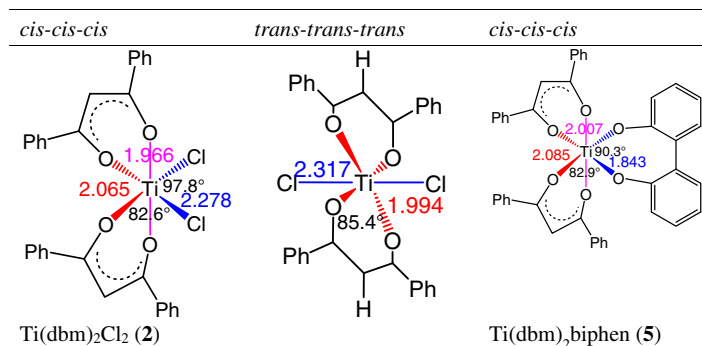


Fig. 7. Selected calculated bond lengths [Å] and angles [°] for $\text{Ti}(\text{dbm})_2\text{Cl}_2$ and $\text{Ti}(\text{dbm})_2\text{biphen}$.

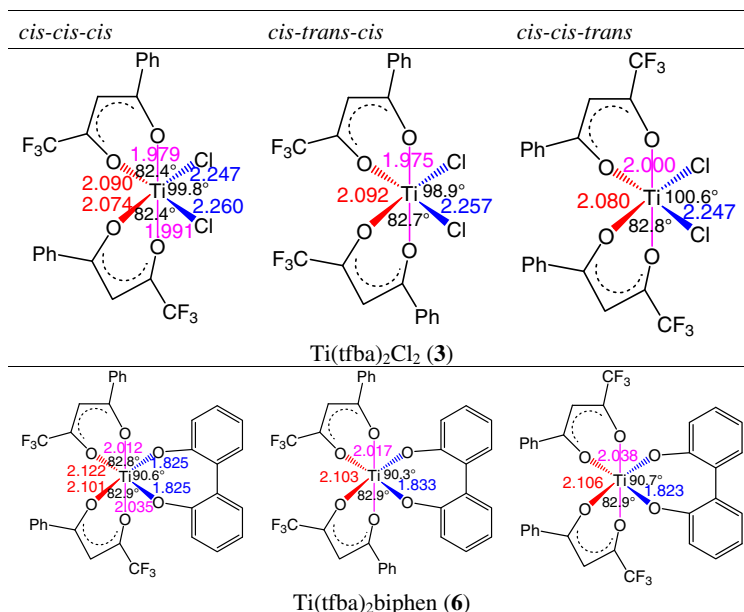


Fig. 8. Selected calculated bond lengths [Å] and angles [°] for $\text{Ti}(\text{tfba})_2\text{Cl}_2$ and $\text{Ti}(\text{tfba})_2\text{biphen}$.

Table 3
Observed and calculated isomer distribution of **1–6**.

Compound	Isomer	% Observed ^1H NMR	% Observed ^{19}F NMR	% Calculated
$\text{Ti}(\text{ba})_2\text{Cl}_2$ (1)	<i>cis-cis-cis</i>	27.9		31.0
	<i>cis-trans-cis</i>	54.7		61.7
	<i>cis-cis-trans</i>	17.4		6.7
	<i>trans-trans-trans</i>	0.0		0.5
	<i>trans-cis-cis</i>	0.0		0.1
$\text{Ti}(\text{dbm})_2\text{Cl}_2$ (2)	<i>cis-cis-cis</i>	100.0		97.1
	<i>trans-trans-trans</i>	0.0		2.9
$\text{Ti}(\text{tfba})_2\text{Cl}_2$ (3)	<i>cis-cis-cis</i>	37.0	32.3	39.5
	<i>cis-trans-cis</i>	38.4	41.9	41.9
	<i>cis-cis-trans</i>	24.6	25.8	18.4
	<i>trans-trans-trans</i>	0.0	0.0	0.2
	<i>trans-cis-cis</i>	0.0	0.0	0.0
$\text{Ti}(\text{ba})_2\text{biphen}$ (4)	<i>cis-cis-cis</i>	25.6		26.5
	<i>cis-trans-cis</i>	49.2		43.7
	<i>cis-cis-trans</i>	25.2		29.8
$\text{Ti}(\text{dbm})_2\text{biphen}$ (5)	<i>cis-cis-cis</i>	100.0		100.0
$\text{Ti}(\text{tfba})_2\text{biphen}$ (6)	<i>cis-cis-cis</i>	17.1	21.2	19.5
	<i>cis-trans-cis</i>	62.4	61.6	62.2
	<i>cis-cis-trans</i>	20.6	17.2	18.3

Table 4
Range of the calculated geometrical parameters (°, Å) for *cis* configured octahedral monomeric complexes **1–6**. Parameters are defined in Fig. 1b.

Compound	d_{ax}	d_{eq}	d_{L}	O–Ti–O	Cl–Ti–Cl or $\text{O}_{\text{L}}\text{–Ti–O}_{\text{L}}$
$\text{Ti}(\beta\text{-diketonato})_2\text{Cl}_2$	1.97–2.00	2.05–2.09	2.25–2.28	82–83	98–101
$\text{Ti}(\beta\text{-diketonato})_2\text{biphen}$	2.00–2.04	2.05–2.12	1.82–1.87	83	90–91

4. Conclusions

Isomerically pure crystals of $\text{Ti}(\text{ba})_2\text{biphen}$ (**4**) have been synthesized. In the solid state **4** adopts the *cis-trans-cis* configuration with the phenyl ends of the benzoylacetonato ligands in the *trans*

position. According to a DFT computational study of the relative energies and abundance of the possible isomers of **4**, this configuration is in agreement with the most stable isomer. A RMSD value of 0.041 Å for the overlay of the calculated and solid state structure of **4** confirms the high degree of accuracy of the computational

method used. The novel Ti(-diketonato)₂biphen complexes are “air stable” and also exhibit high resistance towards hydrolysis.

5. Supplementary material

CCDC No. 702014 contains the supplementary crystallographic data for this paper. These data can be obtained free of charge from The Cambridge Crystallographic Data Centre via www.ccdc.cam.ac.uk/data_request/cif.

Acknowledgements

Financial assistance by the South African National Research Foundation under Grant No. 2067416 and the Central Research Fund of the University of the Free State is gratefully acknowledged.

References

- [1] (a) Y. Qian, J. Huang, M.D. Bala, B. Lian, H. Zhang, H. Zhang, *Chem. Rev.* 103 (2003) 2633;
(b) R. Beckhause, C. Santamaria, *J. Organomet. Chem.* 617 (2001) 81;
(c) E. Manek, D. Hinz, G. Meyer, *Coord. Chem. Rev.* 164 (1997) 5;
(d) J.C. Vites, M.M. Lynam, *Coord. Chem. Rev.* 146 (1995) 1;
(e) J.C. Vites, M.M. Lynam, *Coord. Chem. Rev.* 138 (1995) 71;
(f) R.O. Duthaler, A. Hafner, *Chem. Rev.* 92 (1992) 807.
- [2] E. Meléndez, *Crit. Rev. Oncol. Hematol.* 42 (2002) 309.
- [3] B.K. Keppler, C. Friesen, H.G. Moritz, H. Vongerichten, E. Vogel, *Struct. Bond.* 78 (1991) 97.
- [4] P. Köpf-Maier, *Eur. J. Clin. Pharmacol.* 47 (1994) 1.
- [5] E. Dubler, R. Buschmann, H.W. Schmalte, J. *Inorg. Biochem.* 95 (2003) 97.
- [6] P. Comba, H. Jakob, B. Nuber, B.K. Keppler, *Inorg. Chem.* 33 (1994) 3396.
- [7] B.S. Furniss, A.J. Hannaford, P.W.G. Smith, A.R. Tatchell, in: *Vogel's Textbook of Practical Organic Chemistry*, 5th ed., John Wiley & Sons, New York, 1994, p. 409.
- [8] R.C. Fay, R.N. Lowry, *Inorg. Chem.* 6 (1967) 1512.
- [9] N. Serpone, R.C. Fay, *Inorg. Chem.* 6 (1967) 1835.
- [10] APEX2 (Version 1.0-27), Bruker AXS Inc., Madison, Wisconsin, USA, 2005.
- [11] COSMO (Version 1.48), Bruker AXS Inc., Madison, Wisconsin, USA, 2003.
- [12] SAINT-PLUS (Version 7.12 including XPREP), Bruker AXS Inc., Madison, Wisconsin, USA, 2004.
- [13] SADABS (Version, 2004/1), Bruker AXS Inc., Madison, Wisconsin, USA, 1998.
- [14] A. Altomare, M.C. Burla, M. Camalli, G.L. Cascarano, C. Giacovazzo, A. Guagliardi, A.G.G. Moliterni, G. Polidori, R. Spagna, *J. Appl. Crystallogr.* 32 (1999) 115.
- [15] L.J. Farrugia, *J. Appl. Crystallogr.* 32 (1999) 837. WINGX 1.70.01.
- [16] G.M. Sheldrick, *SHELXL97*, Program for Crystal Structure Refinement, University of Göttingen, Germany, 1997.
- [17] A.J.C. Wilson (Ed.), *International Tables for Crystallography*, vol. C, Kluwer Academic Publishers, Dordrecht, The Netherlands, 1995.
- [18] K. Brandenburg, H. Putz, *DIAMOND Release 3.1a*, Crystal Impact GbR, Bonn, Germany, 2005.
- [19] The ADF program system was obtained from Scientific Computing and Modeling, Amsterdam (<http://www.scm.com/>). For a description of the methods used in ADF, see: G.T. Velde, F.M. Bickelhaupt, E.J. Baerends, C.F. Guerra, S.J.A. van Gisbergen, J.G. Snijders, T.J. Ziegler, *J. Comp. Chem.* 22 (2001) 931.
- [20] J.P. Perdew, J.A. Chevary, S.H. Vosko, K.A. Jackson, M.R. Perderson, D.J. Singh, C. Fiohais, *Phys. Rev. B* 46 (1992) 6671.
- [21] G.A. Zhurko, D.A. Zhurko, *CHEM CRAFT*, Version 1.5 (build 282), 2007.
- [22] O. Kubaschewski, E.L. Evans, C.B. Alcock, *Metallurgical Thermochemistry*, 4th ed., Oxford, UK, 1967. Table A, p. 304.
- [23] B.K. Keppler, M.E. Heim, *Drug Future* 3 (1988) 638.
- [24] P.V. Rao, C.P. Rao, E.K. Wegelius, E. Kolehmainen, K. Rissanen, *J. Chem. Soc., Dalton Trans.* (1999) 4470.
- [25] W.H. Baier, *Acta Crystallogr.* 9 (1956) 515.
- [26] A. Bodner, P. Jeske, T. Weyhermuller, K. Wieghardt, E. Dubler, H. Scmalte, B. Nuber, *Inorg. Chem.* 31 (1992) 3737.
- [27] P. Corradini, S. Allegra, *J. Am. Chem. Soc.* 81 (1959) 5510.
- [28] (a) C. Janiak, *J. Chem. Soc., Dalton Trans.* (2000) 3885;
(b) G.B. McGaughey, M. Gagne, A.K. Rappe, *J. Biol. Chem.* 273 (1998) 15458.
- [29] (a) S.K. Burley, G.A. Petsko, *Science* 229 (1985) 23;
(b) S.K. Burley, G. Petsko, *Adv. Protein Chem.* 39 (1988) 125.
- [30] (a) B.K. Keppler, C. Friesen, H.G. Moritz, H. Vongerichten, E. Vogel, in: B.K. Keppler (Ed.), *Metal Complexes in Cancer Chemotherapy*, VCH, Weinheim, Germany, 1993, p. 297;
(b) D.C. Bradley, C.E. Holloway, *J. Chem. Soc. A* (1969) 282.
- [31] N. Serpone, D.G. Brickley, *Inorg. Chim. Acta* 57 (1982) 211.
- [32] W.J. Hehre, *A Guide to Molecular Mechanisms and Quantum Chemical Calculations*, Wavefunction Inc., 2003. vol. 181, p. 153.